 ©2005 Kvantovaya Elektronika and Turpion Ltd

PACS numbers: 42.65.Jx; 42.65.Re; 42.68.Ay
DOI: 10.1070/QE2005v035n01ABEH002894

Dynamic small-scale self-focusing of a femtosecond laser pulse

V.P. Kandidov, O.G. Kosareva, S.A. Shlenov,
N.A. Panov, V.Yu. Fedorov, A.E. Dormidonov

***Abstract*. The formation of many filaments in a laser pulse with initial perturbations of the intensity propagated in a turbulent atmosphere is studied numerically. It is shown that the competition between nonlinear focuses can slow down the formation of filaments during their propagation. The number of filaments in the turbulent atmosphere increases with distance. Nonstationary interference upon defocusing in a laser plasma leads to the appearance of secondary filaments. The dynamic competition between filaments produced during the pulse shortens their length and the length of plasma channels.**

Keywords: *small-scale self-focusing, femtosecond pulses, filamentation.*

1. Introduction

The phenomenon of small-scale self-focusing attracted the attention of researchers as early as the 1970 – 80s in connection with the problem of amplification of high-power nanosecond pulses in solid-state laser systems [1, 2]. At present interest in this phenomenon is caused mainly by modern problems of femtosecond laser optics. During the propagation of high-power femtosecond laser pulses in gases and condensed media, extended filaments are formed, in which a great part of radiation energy is concentrated [3 – 5]. Filamentation is accompanied by the formation of plasma channels and extremely strong broadening of the frequency spectrum of the pulse. The possibility of using these properties of laser radiation for the development of new methods of the femtosecond laser technology in microphotonics, laser probing of the environment, and remote control of electric discharges is being investigated at present [6].

Filaments are formed due to a combined action of the Kerr self-focusing in a medium and nonstationary aberration defocusing of radiation in the laser-produced plasma. In giga- and terawatt pulses, a chaotic beam of filaments is formed, which are produced due to a small-scale self-focusing of laser radiation. The stochasticity of the beam containing many filaments in a femtosecond laser pulse is caused by the spatial instability of an intense light field in a medium with the Kerr nonlinearity [7]. The perturbations of the intensity and phase of the output laser radiation and fluctuations of the refractive index of the medium lead to a random from pulse to pulse location of filaments in the beam, resulting in an irregular backscattering signal in a femtosecond lidar [8].

From the point of view of nonlinear optics, filaments are the traces of moving focuses [9]. Unlike the self-focusing of nanosecond pulses in optical glasses, an increase in the intensity in nonlinear focuses of femtosecond pulses is limited not by two-photon absorption but nonlinear refraction in a laser plasma produced due to multiphoton and tunnel ionisation [10, 11].

Filamentation is detected with a CCD camera as many 'hot' dots appearing in the distribution of the energy density in each pulse or as a supercontinuum generated in experiments. In [12, 13], 42-fs, 40-mJ pulses from a Ti : sapphire laser decomposed during propagation over 35 m into 6 – 8 filaments, which originated from a small number of inhomogeneities in the energy density distribution at the output mirror of the laser system. In the Teramobile setup [14], more than 20 filaments were observed in a 600-fs, 230-mJ pulse at a distance of 55 m. As the pulse duration was reduced down to 100 fs and the peak pulse power increased correspondingly up to 2 TW, first a few tens of filaments appeared of length more than ten metres, which then decomposed into a few hundreds of small-scale 'hot' dots in the energy density distribution in the beam cross section [15].

Theoretically, filamentation was studied by solving numerically a system of equations for slowly varying amplitude of the light field and the electron concentration in the laser-induced plasma [12, 13, 16]. The problem of stochastic formation of many tens and hundreds of filaments in a terawatt pulse in its full formulation with the dimensionality 3D+1, when the nonstationary cubic nonlinearity, material dispersion, and fluctuations of the refractive index of the medium are taken into account, requires an extremely large computational power and cannot be solved even at powerful computer centres containing up to 128 processors [15]. The authors of paper [16] obtained the spatiotemporal picture of the development of filaments in a pulse in which large-scale harmonic perturbations were superimposed on the Gaussian distribution. The decomposition and merging of the initially formed filaments was interpreted as optical turbulence.

V.P. Kandidov, O.G. Kosareva, S.A. Shlenov, N.A. Panov, V.Yu. Fedorov, A.E. Dormidonov Department of Physics, M.V. Lomonosov Moscow State University, Vorob'evy gory, 119992 Moscow, Russia;
e-mail: shlenov@msulic.phys.msu.su

Received 30 September 2004
Kvantovaya Elektronika **35** (1) 59 – 64 (2005)
Translated by M.N. Sapozhnikov

The development of many filaments from two perturbations in the intensity distribution at the laser system output was studied in [13] to explain the fading of a backscattering signal during periodically pulsed probing of the air. The stochastic formation of many filaments during propagation of laser pulses in the turbulent atmosphere was considered in [17] in the quasi-stationary approximation using a phenomenological model of the intensity limitation in moving focuses. In [15], a reduced model was used in which the electron concentration in the plasma channel was calculated by approximating the temporal profile of a pulse in the vicinity of a nonlinear focus by a hypothetical Gaussian peak with a specified duration. This reduced the dimensionality of the problem and allowed the calculation of the energy density distribution in the beam cross section upon filamentation of femtosecond pulses with parameters close to those generated on the Teramobile setup.

In this paper, we study numerically the dynamic small-scale self-focusing of a femtosecond laser pulse, which is manifested in the formation of many filaments. We considered the development of filaments during the propagation of a pulse with a small number of initial perturbations in a regular medium and of an initially unperturbed pulse in the turbulent atmosphere.

2. Model of the filament formation

A pulse of duration $10^{-13} - 10^{-14}$ s can be described in the slowly varying amplitude approximation, and its envelope $E(x, y, z, t)$ in the current time t satisfies the equation

$$2ik\frac{\partial E}{\partial z} = \frac{\partial^2 E}{\partial x^2} + \frac{\partial^2 E}{\partial y^2} + \frac{2k^2}{n_0}(\Delta n_\mathrm{k} + \Delta n_\mathrm{p} + \Delta\tilde{n})E. \qquad (1)$$

The increment Δn_k of the refractive index describes the Kerr nonlinearity. The electron component of this nonlinearity is instantaneous, while the setting time of the response caused by stimulated scattering by rotational transitions of gas molecules is comparable with the pulse duration. Therefore, Δn_k is represented by the convolution [18, 19]

$$\Delta n_\mathrm{k}(t) = \frac{1}{2}n_2\left[|E(t)|^2 + \int_{-\infty}^{t} h(t-t')|E(t')|^2 \mathrm{d}t'\right], \qquad (2)$$

where n_2 is the Kerr nonlinearity coefficient upon quasi-stationary radiation. For the air, the response function $h(t)$ can be approximated by the expression [18]

$$h(t) = \mathrm{step}(t)\Omega^2 \exp\left(-\frac{\Gamma t}{2}\right)\frac{\sin(\Lambda t)}{\Lambda}, \qquad (3)$$

where $\Lambda^2 = \Omega^2 - (\Gamma^2/4)$; $\Omega = 20.6$ THz; and $\Gamma = 26$ THz.

The contribution Δn_p of the laser plasma to the nonlinearity is determined by the frequency $\nu_\mathrm{c} = N_0 \upsilon_\mathrm{e}\sigma_\mathrm{c}$ of collisions with neutral particles of the medium and by the plasma frequency $\omega_\mathrm{p} = (4\pi e^2 N_\mathrm{e}/m_\mathrm{e})^{1/2}$:

$$\Delta n_\mathrm{p} = -\frac{\omega_\mathrm{p}^2}{2n_0(\omega^2 + \nu_\mathrm{c}^2)}\left(1 - \mathrm{i}\frac{\nu_\mathrm{c}}{\omega}\right), \qquad (4)$$

where e and m_e are the electron charge and mass, respectively; N_0 is the concentration of neutral particles; υ_e is the electron velocity; σ_c is the cross section for collisions of electrons with neutral particles; ω is the laser radiation frequency; and n_0 is the refractive index of the medium. A change in the electron concentration is described by the kinetic equation

$$\frac{\partial N_\mathrm{e}}{\partial t} = R(|E|^2)(N_0 - N_\mathrm{e}) + \nu_\mathrm{i} N_\mathrm{e} - \beta N_\mathrm{e}^2, \qquad (5)$$

where β is the recombination rate. The rate of multiphoton ionisation was determined using the Perelomov–Popov–Terent'ev model [20] for calculating the rate of avalanche ionisation, which plays an important role in condensed media. This rate is [21]

$$\nu_\mathrm{i} = \frac{1}{W}\frac{e^2E^2}{2m_\mathrm{e}(\omega^2 + \nu_\mathrm{c}^2)}\nu_\mathrm{c}, \qquad (6)$$

where W is the ionisation potential (the energy gap width).

Fluctuations of the refractive index $\Delta\tilde{n}(x, y, z)$ in the medium are determined by the spatial spectrum $F_{\Delta n}$, which for the atmospheric turbulence has the form [22]

$$F_{\Delta n}(\kappa_x, \kappa_y, \kappa_z) = 0.033C_n^2(\kappa^2 + \kappa_0^2)^{-11/6}\exp(-\kappa^2/\kappa_m^2),$$

$$\kappa^2 = \kappa_x^2 + \kappa_y^2 + \kappa_z^2, \qquad (7)$$

where the parameter C_n^2 characterises the magnitude of turbulent fluctuations and the constants $\kappa_0 = 2\pi/L_0$ and $\kappa_m = 5.92/l_0$ give the lower and upper boundaries of spatial frequencies of the inertial interval of turbulence [from the external (L_0) to internal (l_0) scale].

Model (1) neglects the wave instability, which results in a nonlinear increase in the slope of pulse fronts [23] and does not affect the formation of nonlinear focuses in its cross section. In addition, (1) does not contain the group-velocity dispersion, because the dispersion length of pulses under study exceeds the distance over which the spatial instability develops [24].

3. Pulse with intensity perturbations in a regular medium

Consider the formation of filaments in a pulse with initial intensity perturbations for a superposition of two partial coherent beams, whose centres are displaced with respect to each other in the cross section plane. We assume that the partial beams are Gaussians with equal amplitudes and widths:

$$E(x, y, z = 0, \tau) = \exp\left(-\frac{\tau^2}{2\tau_0^2}\right)E(x, y),$$

$$E(x, y) = E_0\exp\left[-\frac{(y - d/2)^2 + x^2}{2a_0^2}\right]$$

$$+ E_0\exp\left[-\frac{(y + d/2)^2 + x^2}{2a_0^2}\right], \qquad (8)$$

where d is the distance between the partial beams of radius a_0. This model corresponds to the energy density distribution observed at the output of a femtosecond laser system [25]. As a scale for the peak power P of the pulse (8), we can use the critical self-focusing power of a Gaussian beam

$$P_g = \frac{\pi n_0}{2k^2 n_2} R_{cr},$$

which is close to the power of the Townes mode describing the field in a nonlinear focus [26]. The nonlinearity parameter R_{cr} was estimated as $R_{cr}^{ax} = 1$ in the axial approximation [27], $R_{cr}^{H} = 4$ by equating the beam Hamiltonian H to zero [28], and $R_{cr}^{cs} = 3.77$ according to numerical simulation [29].

The appearance and the initial stage of formation of filaments are determined by the Kerr self-focusing of radiation during which the radiation intensity in nonlinear focuses increases up to the ionisation threshold of the medium. (In the air at the atmospheric pressure, the multiphoton ionisation threshold is $\sim 5 \times 10^{13}$ W cm^{-2} [30], in water this threshold is 10^{13} W cm^{-2} [31].) Plasma in a nonlinear focus causes the defocusing of the subsequent temporal slices of the pulse, resulting in the appearance of interference rings in the distributions of the intensity and energy density [11]. The plasma channel stabilises the parameters being measured, which characterise the filament energy and transverse size. Strong gradients of the light field in the plasma cause the generation of a supercontinuum [32].

To analyse qualitatively the initial stage of the filament formation, we consider the stationary self-focusing of laser radiation (8), whose intensity coincides with the peak pulse intensity. It follows from numerical calculations that in this case two critical powers $P_{cr}^{(1)}$ and $P_{cr}^{(2)}$ exist, whose values depend on the distance d between the partial beams (Fig. 1a). For the peak power $P < P_{cr}^{(1)}$, filaments are absent. For $P_{cr}^{(1)} < P < P_{cr}^{(2)}$, one nonlinear focus appears in the pulse and, hence, one filament forms. For $P > P_{cr}^{(2)}$, two and more filaments appear. For $d \to \infty$, the radiation decomposes into two uncoupled partial beams, the values of $P_{cr}^{(1)}$ and $P_{cr}^{(2)}$ tend to $2P_g^{cs}$, and one filament can no longer be formed.

As the peak power P increases, the displacement of partial beams being constant ($d/a_0 = \text{const}$), the distance Z_f to the filament origin changes nonmonotonically. When the first critical power is slightly exceeded [$P \geqslant P_{cr}^{(1)}$], the distance Z_f rapidly decreases with increasing P. For $P > P_{cr}^{(1)}$, this decrease slows down, and as the power P approaches $P_{cr}^{(2)}$, the self-focusing distance Z_f increases with P (Fig. 1b). Such a type of the dependence $Z_f(P)$ is explained by a competition between initial perturbations, which can be treated as 'stationary' because it develops with the distance z and is independent of time t. For the peak power $P \geqslant P_{cr}^{(1)}$, the initial perturbations at the beginning of propagation merge into one, and then self-focusing occurs, at which the power from the beam periphery transfers to its axis according to the model of moving focuses [33]. In this case, the distance to the filament origin decreases with increasing P. For $P \leqslant P_{cr}^{(2)}$, initial perturbations first increase independently. Then, the 'extended' competition occurs between the enhanced perturbations, and the power accumulated in them transfers to the beam axis, where one nonlinear focus forms. The 'stationary' redistribution of power in the pulse cross section increases the time of the pulse formation, and the distance to the pulse origin increases. For $P > P_{cr}^{(2)}$, the distance Z_f again monotonically decreases with increasing power.

The first critical power $P_{cr}^{H^{(1)}}$ was analytically estimated by equating the Hamiltonian to zero (Fig. 1a) [34]. It follows from the dependence of $P_{cr}^{H^{(1)}}/P_g^H$ on the distance

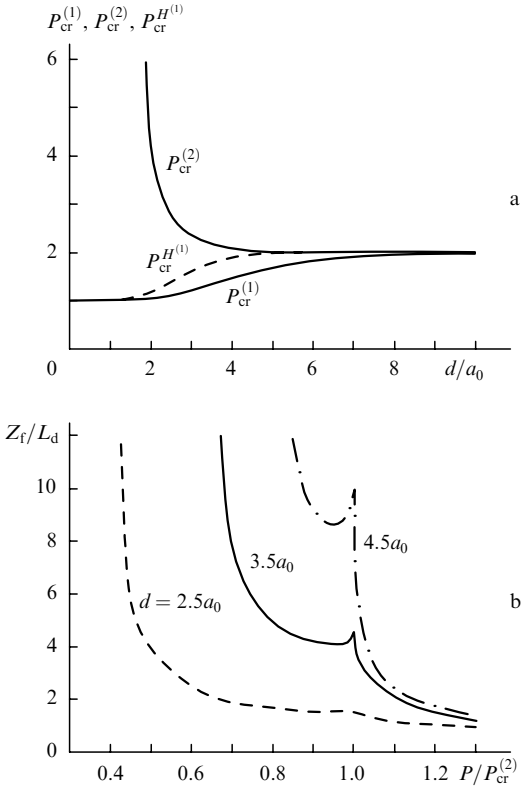

Figure 1. Dependences of the critical powers $P_{cr}^{(1)}$ and $P_{cr}^{(2)}$ on the distance d between the maxima of perturbations in the initial intensity distribution and the estimate of $P_{cr}^{H(1)}$ from the Hamiltonian ($P_{cr}^{(1)}$ and $P_{cr}^{(2)}$ are normalised to the critical self-focusing power P_g^{cs} of the Gaussian beam calculated numerically, $P_{cr}^{H^{(1)}}$ is normalised to the critical power P_g^H calculated from the Hamiltonian) (a) and dependences of the distance Z_f to the filament origin on the peak power P for different distances between initial perturbations d ($L_d = ka_0^2$ is the diffraction length of the partial beam) (b).

d that the estimate by the Hamiltonian H gives the overestimated critical power in the region $d/a_0 = 2 - 6$, where the nonlinear focus is formed during a strong competition between initial perturbations.

We considered dynamic self-focusing during the propagation of a 27-fs pulse (8) in water with partial beams of radius $a_0 = 63$ μm separated by the distance $d = 2a_0$. These parameters correspond to the experiment on filamentation of a pulse focused in water [35]. The Kerr nonlinearity in water can be treated as inertialless, and the response function $h(t)$ can be represented by the delta function $\delta(t)$. The nonlinearity coefficient for water is $n_2 = 10^{-19}$ cm^2 W^{-1}, which corresponds to the critical self-focusing power of a Gaussian beam $P_g = 4 \times 10^6$ W [35]. Avalanche ionisation in water makes a substantial contribution to the plasma production because for the radiation intensity in the filament equal to $10^{13} - 10^{14}$ W cm^{-2}, the ionisation rate ν_i achieves $\sim 5/\tau_0$, while the collision frequency ν_c is close to the radiation frequency ω_0. The distributions of the energy density $J(x, y)$ in the pulse cross section and the electron concentration $N_e(x, y)$ in the plasma are presented in the form of tinted images in Fig. 2 for different distances z. Initially, $J(x, y)$ has the distribution with two weak maxima, which is elongated along the y axis (Fig. 2a). For the peak power $P = 5.3 \times 10^8$ W, which, according to the depen-

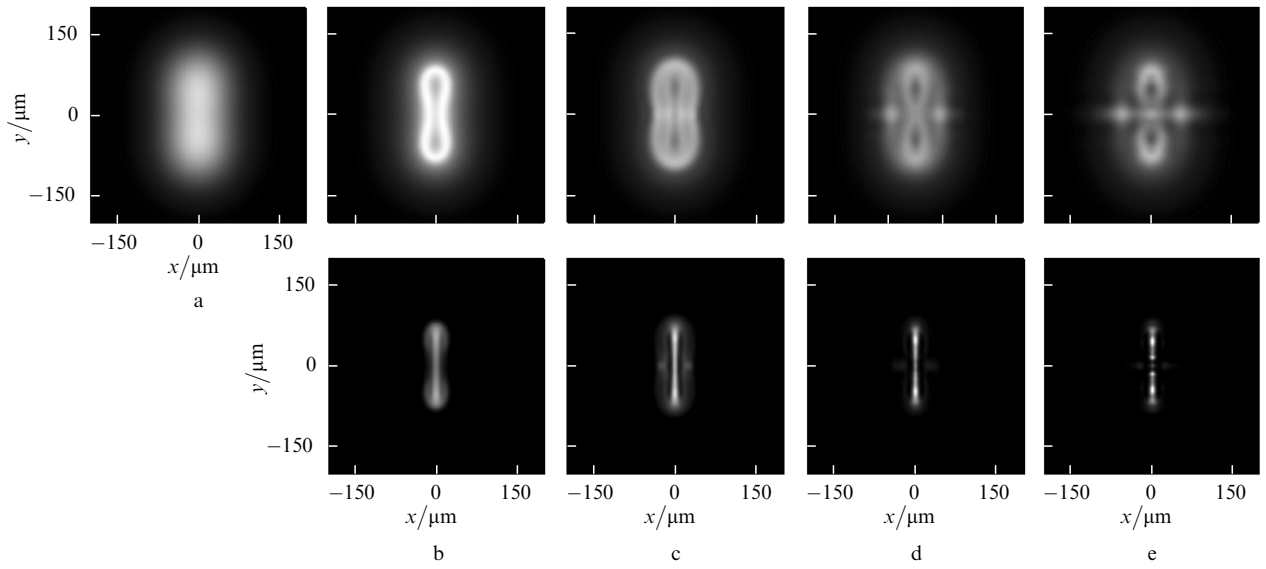

Figure 2. Tinted images of the distributions of the energy density (upper row) and the electron density $N_e(x, y)$ in a laser plasma (lower row) in the pulse cross section at distances $z/L_d = 0$ (a), 0.15 (b), 0.20 (c), 0.25 (d), and 0.30 (e). The energy density J is normalised to 0.29 J cm^{-2}, the electron density N_e is normalised to 2.7×10^{19} cm^{-3}.

dence in Fig. 1a, is lower than $P_{cr}^{(2)}$ but is higher than $P_{cr}^{(1)}$, one filament forms in the pulse with a plasma channel at the axis.

In a pulse with the energy $W = 140$ μJ and peak power $P = 3 \times 10^9$ W exceeding $P_{cr}^{(2)}$, two closely spaced filaments are formed in the plane $z = 0.15L_d$, where $L_d = ka_0^2$ is the diffraction length of the partial beam (Fig. 2b). The radiation intensity between the filaments achieves the photoionisation threshold, and a connector appears between the plasma channels. Defocusing in the plasma produces waves at the rear edge of the pulse, which go away from the filaments, carrying their power. This results in the appearance of local minima at the centres of filaments in the energy density distribution. At the distance $z = 0.20L_d$, the interference of these waves leads to the formation of the intensity maxima, at which two short secondary filaments appear (Fig. 2c). Later (for $z = 0.25L_d$), the local maxima of the energy density are preserved at the place of secondary ones. However, plasma channels disappear because the radiation intensity does not achieve the ionisation threshold during the pulse (Fig. 2d) and two filaments with a complex energy density distribution remain. The cross section of their plasma channels are elongated (Fig. 2e).

4. Pulse in the turbulent atmosphere

The frequency of collisions of electrons with neutral particles in the air for the radiation intensity achieved in a filament is about 2×10^{12} s^{-1}, and the contribution of avalanche ionisation to the plasma production during the propagation of pulses of duration shorter than 500 fs is negligible. In addition, we can neglect electron recombination, which occurs for ~ 1 ns. The critical self-focusing power for pulses of duration 10^{-13} fs is 6×10^9 W according to measurements [5].

Filamentation in the presence of fluctuations of the refractive index of the air was considered for a 100-fs, 0.8 μm pulse with the peak energy density $J_0 = 8$ mJ cm^{-2}. The radiation intensity was described by the unimodal Gaussian distribution ($d = 0$) with the width $a_0 = 0.92$ cm and the maximum value $I_0 = 0.45 \times 10^{11}$ W cm^{-2}. The fluctuations of the refractive index along the path were simulated by a phase screen, whose statistical characteristics corresponded to the atmospheric turbulence with the parameters $C_n^2 = 2 \times 10^{-15}$ cm$^{-2/3}$, $L_0 = 1$ m, and $l_0 = 1$ mm.

The dynamics of the intensity distribution $I(x, y)$ over the pulse cross section is illustrated in Fig. 3, where the tinted images of $I(x, y)$ are presented for different times t and $z = 80$ m. At the leading edge of the pulse ($t/\tau_0 = -0.8$) in the central part of the beam in the region of a 'focusing' fluctuation of the refractive index in the turbulent atmosphere, a nonlinear focus arises (Fig. 3a). In the temporal slice $t/\tau_0 = -0.4$, defocusing is observed in the plasma produced by the previous slices of the pulse. At the centre of the produced filament a local intensity minimum appears (Fig. 3b). In addition, the interference of the wave going away from the filament and the incident wave, perturbed by atmospheric fluctuations, results in the formation of the stochastic picture of the intensity maxima in which the ring structure is manifested, which is observed in homogeneous media [11]. The intensity maxima become the centres of the formation of secondary filaments in the next temporal slices. In the central temporal slice ($t/\tau_0 = 0$), the number of global maxima and local maxima, caused by the interference of the waves, increases (Fig. 3c). At the pulse tail, where power decreases, defocusing in the laser plasma is especially prominent, and only weak and blurred intensity perturbations remain in the pulse cross section, whose number decreases (Figs 3d, e). Note that the positions of the intensity maxima in the (x, y) plane change during the pulse because they depend on the perturbations of the refractive index caused by the turbulence and plasma produced by previous filaments.

Figure 4 shows a change in the distributions of the energy density $J(x, y)$ and electron concentration $N_e(x, y)$ in plasma with the distance z. At the distance $z = 50$ m, one can see a 'hot dot' of the primary filament with a high energy density (Fig. 4a) and the corresponding plasma channel with a drastically increased electron concentration

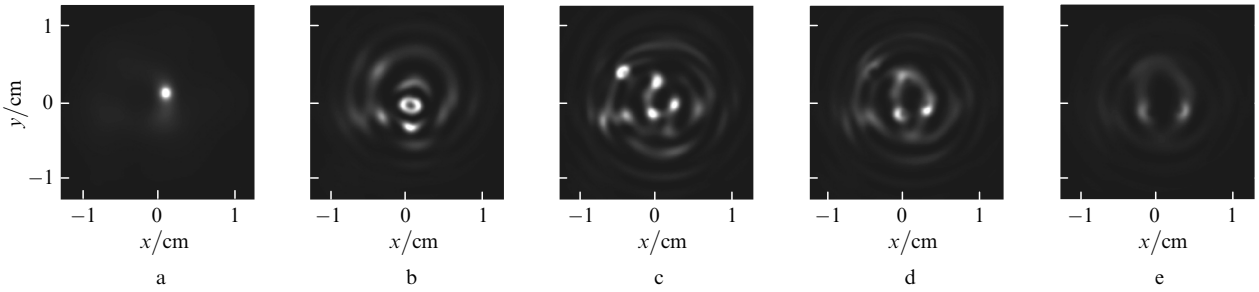

Figure 3. Intensity distribution $I(x, y)$ in the pulse cross section at the distance $z = 80$ m in the turbulent atmosphere for the peak pulse power $P = 20P_{cr}$. Sections correspond to the instants $t/\tau_0 = -0.8$ (a), -0.4 (b), 0 (c), and 0.8 (d).

(Fig. 4d). Also, perturbations in the energy density distribution caused by the atmospheric turbulence exist, in which the probability of the formation of new filaments is high. As a result, another 'hot dot' appears at a distance of 60 m, which corresponds to the secondary filament (Fig. 4b), and the number of plasma channels increases (Fig. 4e). The plasma produced by the primary filament leads to the formation of a local minimum at the filament axis and of a ring structure in the distribution $J(x, y)$.

Later on, the pulse decomposes into many randomly located filaments and plasma channels (Figs 4c, f). In this case, the positions of these channels in the pulse cross section can be not coincident with 'hot dots' in the energy density distribution. As follows from analysis of the dynamics of plasma channels, during refraction a local tilt of the wave front appears in them, resulting in the appearance of weakly diverging trajectories of filaments and in a noticeable displacement of plasma channels along the extended atmospheric path.

5. Conclusions

In a high-power femtosecond laser pulse, dynamic self-focusing develops, resulting in the formation of many filaments in the pulse cross section. A stationary competition between nonlinear focuses at the initial stage of filamentation can lead to an increase in the distance to the filament origin. The intensity maxima in the nonstationary interference pattern produced due to defocusing of filaments in the laser plasma are the centres of the formation of secondary filaments. Fluctuations of the refractive index in the turbulent atmosphere result in an irregular interference pattern and stochastic decay of the pulse into numerous filaments. The direction of the power transfer in the pulse cross section varies with time during the formation of filaments. The dynamic competition between filaments affects their length and the length of plasma channels.

Acknowledgements. This work was supported by the Russian Foundation for Basic Research (Grant No. 03-02-16939) and the European Office of Scientific Research of the USA Army (Contract No. 62558-03-M-0029).

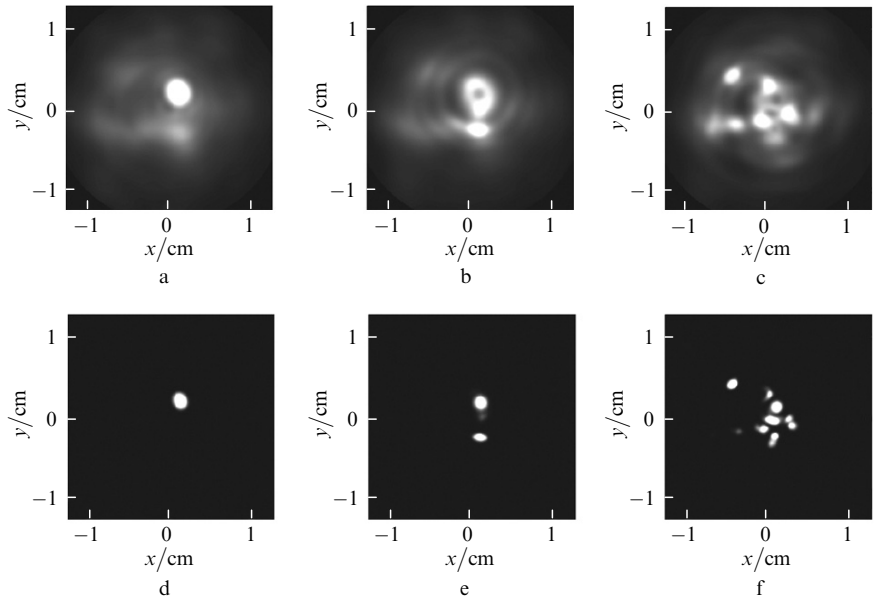

Figure 4. Distributions of the energy density $J(x, y)$ (a – c) and the electron density $N_e(x, y)$ in the laser plasma (d – f) in the pulse cross section in the turbulent atmosphere at distances $z = 50$ (a, d), 60 (b, e), and 80 m (c, f). The energy density J is normalised to 14 mJ cm^{-2}, the electron density N_e is normalised to 2×10^{14} cm^{-3}.

References

1. Zherikhin A.N., Matveets Yu.A., Chekalin S.V. *Kvantovaya Elektron.*, **3**, 1585 (1976) [*Sov. J. Quantum Electron.*, **6**, 858 (1976)].
2. Baranova N.B., Bykovskii N.E., Senatskii Yu.V., Chekalin S.V. *Trudy FIAN*, **103**, 84 (1978).
3. Braun A., Korn G., Liu X., Du D., Squi J., Mourou G. *Opt. Lett.*, **20**, 73 (1995).
4. Nibbering E.T.J., Curley P.F., Grillon G., Prad B.S., Franco M.A., Salin F., Mysyrowicz A. *Opt. Lett.*, **1**, 62 (1996).
5. Brodeur A., Chien C.Y., Ilkov F.A., Chin S.L., Kosareva O.G., Kandidov V.P. *Opt. Lett.*, **22**, 304 (1997).
6. Kasparian J., Rodrigues M., Mejean G., Yu J., Salmon E., Wille H., Bourayou R., Frey S., Andre Y.-B., Mysyrowicz A., Souerbrey R., Wolf J.-P., Wöste L. *Science*, **301**, 61 (2003).
7. Bespalov V.I., Litvak A.G., Talanov V.I., in *Nelineinaya optika* (Nonlinear Optics) (Novosibirsk: Nauka, 1968).
8. Luo Q., Liw W., Chin S.L. *Appl. Phys. B*, **76**, 1 (2002).
9. Lugovoi V.N., Prokhorov A.M. *Pis'ma Zh. Eksp. Teor. Fiz.*, **7**, 153 (1968).
10. Kosareva O.G., Kandidov V.P., Brodeur A., Chin S.L. *J. Nonlinear Opt. Phys.*, **6**, 485 (1997).
11. Chin S.L., Petit S., Liu W., Iwasaki A., Nadeu M.C., Kandidov V.P., Kosareva O.G., Andrianov K.Yu. *Opt. Commun.*, **210**, 329 (2002).
12. Liu W., Hosseini S.A., Luo Q., Ferland B., Chin S.L., Kosareva O.G., Panov N.A., Kandidov V.P. *New J. Phys.*, **6** (6), 1 (2004).
13. Hosseini S.A., Luo Q., Ferland B., Liu W., Chin S.L., Kosareva O.G., Panov N.A., Aközbek N., Kandidov V.P. *Phys. Rev. A*, **70**, 033802-1 (2004).
14. Wille H., Rodriguez M., Kasparian J., Mondelain D., Yu J., Mysyrowicz A., Sauerbrey R., Wolf J.P., Wöste L. *Eur. Phys. J.–Appl. Phys.*, **20**, 183 (2002).
15. Berge L., Skupin S., Lederer F., Mejean G., Yu J., Kasparian J., Salmon E., Wolf J.P., Rodriguez M., Wöste L., Bourayou R., Sauerbrey R. *Phys. Rev. Lett.*, **92**, 225002-1 (2004).
16. Mlejnek M., Kolesik M., Moloney J.V., Wright E.M. *Phys. Rev. Lett.*, **83**, 2938 (1999).
17. Shlenov S.A., Kandidov V.P. *Atmos. Oceanic Opt.*, **17**, 630 (2004).
18. Mlejnek M., Wright E.M., Moloney J.V. *Opt. Lett.*, **23**, 382 (1998).
19. Oleinikov P.A., Platonenko V.T. *Laser Phys.*, **3**, 618 (1993).
20. Perelomov A.M., Popov V.S., Terent'ev M.V. *Zh. Eksp. Teor. Fiz.*, **50**, 1393 (1966).
21. Raizer Yu.P. *Gas Discharge Physics* (New York, Berlin: Springer-Verlag, 1991; Moscow: Nauka, 1992).
22. Zuev V.E., Banakh V.A., Pokasov V.V. *Optika turbulentnoi atmosphery* (Optics of Turbulent Atmosphere) (Leningrad: Gidrometeoizdat, 1988).
23. Akhmanov S.A., Vysloukh V.A., Chirkin A.S. *Optics of Femtosecond Laser Pulses* (New York: AIP, 1992; Moscow: Nauka, 1988).
24. Kosareva O.G., Panov N.A., Kandidov V.P. *Atmos. Oceanic Opt.*, in press.
25. Andrianov K.Yu., Kandidov V.P., Kosareva A.G., Chin S.L., Talebpur A., Petin S., Lou V., Ivasaki A., Nade M.-K. *Izv. Ross. Akad. Nauk, Ser. Fiz.*, **66**, 1091 (2002).
26. Fibich G., Gaeta A.L. *Opt. Lett.*, **25**, 335 (2000).
27. Akhmanov S.A., Sukhorukov A.P., Khokhlov R.V. *Usp. Fiz. Nauk*, **93**, 19 (1967).
28. Zakharov V.E., Sobolev V.V., Synakh V.S. *Zh. Eksp. Teor. Fiz.*, **60**, 136 (1971).
29. Marburger J.H., in *Progr. Quantum Electron.*, **4**, 35 (1975).
30. Wood W.M., Siders C.W., Downer M.C. *IEEE Trans. Plasma. Sci.*, **21**, 20 (1993).
31. Feng Q., Moloney J.V., Newell A.C., Wright E.M., Cook K., Kennedy P.K., Hammer D.X., Rockwell B.A., Thompson C.R. *IEEE J. Quantum Electron.*, **33**, 127 (1997).
32. Kandidov V.P., Kosareva O.G., Golubtsov I.S., Liu W., Becker A., Aközbek N., Bowden C.M., Chin S.L. *Appl. Phys. B*, **77**, 149 (2003).
33. Dyshko A.L., Lugovoi V.N., Prokhorov A.M. *Pis'ma Zh. Eksp. Teor. Fiz.*, **6**, 655 (1967).
34. Berge L., Schmidt M.R., Rasmussen J.J., Christansen P.L., Rasmussen K.O. *J. Opt. Soc. Am.*, **14**, 2550 (1997).
35. Liu W., Kosareva O.G., Golubtsov I.S., Iwasaki A., Becker A., Kandidov V.P., Chin S.L. *Appl. Phys. B*, **76**, 1 (2003).